Marine Pollution Bulletin 207 (2024) 116830

Contents lists available at ScienceDirect

Marine Pollution Bulletin

journal homepage: www.elsevier.com/locate/marpolbul

# Mitigation of hypoxia and ocean acidification on the inner East China Sea shelf impacted by the 2023 summer drought

Shiping Lei [a], Dezhi Bu [a], Xianghui Guo [a,b,*], Yi Xu [a], Yi Yang [a], Shuqi An [a], Yan Li [a], Jinyan Pang [a], Kuanbo Zhou [a]

[a] State Key Laboratory of Marine Environmental Science, College of Ocean and Earth Sciences, Xiamen University, Xiamen 361102, China
[b] Fujian Provincial Key Laboratory for Coastal Ecology and Environmental Studies, Xiamen University, Xiamen 361102, China

ARTICLE INFO

*Keywords:*
Changjiang estuary
Summer drought
Mitigation
Hypoxia
Acidification

ABSTRACT

Hypoxia and acidification are universal environmental issues in coastal seas, especially in large river dominated shelves, and the East China Sea shelf is a typical case among them. However, the responses of status of hypoxia and acidification in coastal seas to the extremes of river discharges are still to be revealed. This study surveyed the influences of a summer drought on the status of hypoxia and acidification on the inner East China Sea shelf off the Changjiang estuary. In August of 2023 during a summer drought, carbonate system parameters and dissolved oxygen (DO) were surveyed on the East China Sea shelf off the Changjiang estuary. As expected, dissolved inorganic carbon (DIC) removal (up to >40 μmol $kg^{-1}$) and DO over-saturation (up to >110 %) accompanied by high pH (up to >8.15) in the surface water were observed. However, low DO (32–172 μmol $kg^{-1}$), low pH (7.63–8.04) and low saturation state index of aragonite ($\Omega_{Ar}$) (1.34–3.06) in the bottom water were observed. Relationships of Excess DIC with DO consumption, and pH and $\Omega_{Ar}$ with Excess DIC indicated that the hypoxia and acidification in the bottom water was due mainly to the remineralization of the marine-sourced organic matter. Nevertheless, both hypoxia and acidification were mitigated, i.e. the hypoxic area was smaller, the minimum DO concentration, pH and saturation state index of aragonite were higher in August of 2023 than under the general summer condition. The lower Changjiang discharge (~60 % of the long-term monthly average) mitigated eutrophication of the East China Sea shelf and decreased the phytoplankton biomass in the surface water and subsequently the hypoxia and acidification in the bottom water. However, acidification of the bottom water on the East China Sea shelf was still severe even during the summer drought. Regulating the anthropogenic impact on the coastal marginal seas is still urgently needed to mitigate the acidification status.

## 1. Introduction

Hypoxia and acidification in estuaries and coasts are universal environmental problems in the recent decades (Caballero-Alfonso et al., 2015; Feely et al., 2018; Fennel and Testa, 2019; Rabalais et al., 2010; Zhao et al., 2020). The northern Gulf of Mexico, the East China Sea shelf, the Pearl River estuary and the Baltic Sea, etc., are well-known cases (Carstensen et al., 2014; Li et al., 2002; Rabalais et al., 2010; Rabalais et al., 2002; Wang et al., 2016; Zhao et al., 2020).

In large river estuaries and adjacent coastal areas, eutrophication due mainly to riverine input, stimulates primary production, and increases the marine sourced organic matter production and subsequently fuels dissolved oxygen consumption in bottom water (Carstensen et al., 2014; Rabalais et al., 2010; Zhao et al., 2020). Eutrophication induced bottom water hypoxia usually companied by enhanced ocean acidification (much more severe than the acidification induced by atmospheric $CO_2$ invasion), such as the northern Gulf Mexico, the East China Sea, the Puget Sound (an urbanized estuary), the St. Lawrence estuary, and the coast off Oregon, etc. (Cai et al., 2011; Chou et al., 2013; Feely et al., 2010; Guo et al., 2021; Grantham et al., 2004; Jiang et al., 2019; Jutras et al., 2020).

The East China Sea is a typical marginal sea influenced by large river (the Changjiang). Hypoxia in the bottom water of the East China Sea shelf was found for the first time in August of 1999 (Li et al., 2002). Since then, development and maintenance mechanism of hypoxia has become a research hotspot for more than two decades (Wang et al., 2012; Wang et al., 2016; Wang et al., 2017; Wang et al., 2021; Wei et al., 2007; Xu et al., 2020b; Zhang et al., 2016; Zhang et al., 2018, 2019, 2023; Zhou

* Corresponding author at: Fujian Provincial Key Laboratory for Coastal Ecology and Environmental Studies, Xiamen University, Xiamen 361102, China.
*E-mail address:* xhguo@xmu.edu.cn (X. Guo).

https://doi.org/10.1016/j.marpolbul.2024.116830
Received 21 June 2024; Received in revised form 4 August 2024; Accepted 6 August 2024

et al., 2017; Zhu et al., 2017; Zhu et al., 2023). Usually hypoxic area covers 5000–20,000 km$^2$ (Li et al., 2002; Wang et al., 2021; Zhou et al., 2017). Strong organic matter remineralization as a sequence of eutrophication and the strong stratification are the important processes producing summer bottom water hypoxia (Ni et al., 2016; Wang et al., 2016; Wang et al., 2017).

In the bottom water of the East China Sea shelf, Cai et al. (2011) found that the eutrophication induced acidification in the bottom water of the East China Sea shelf is 0.29 of pH decrease, which is much higher than the $CO_2$-invation induced acidification (0.11 of pH decrease). Subsequently, Chou et al. (2013) found that the saturation state index of aragonite in the bottom water of the East China Sea shelf ranged 1.7–3.2 in the summer of 2009. Xiong et al. (2020) report the saturation state index of aragonite to be 1.2–1.4 in the hypoxic bottom water in the East China Sea off the Changjiang estuary in the summer of 2018.

The Changjiang discharge is an important factor regulating the primary production and the hypoxia status on the East China Sea shelf (Liu et al., 2015; Zhang et al., 2023). However, the response of field observed status of acidification to the extremes of the Changjiang discharge has not been reported.

Average monthly summer discharge from the Changjiang is $2.0\times10^4$ to $7.1\times10^4$ m$^3$ s$^{-1}$, with long-term seasonal average of $4.4\times10^4$ m$^3$ s$^{-1}$. However, the lower Changjiang drainage basin was very dry from spring to summer of 2023, and monthly average freshwater discharge from June to August ranged $2.6\times10^4$ to $3.0\times10^4$ m$^3$ s$^{-1}$, which were only ~60 % of the long-term monthly average (Fig. S1). How the status of hypoxia and acidification responses to the summer drought is a common concern. In this study, based on comparison with August of 2016, we report the mitigated status of hypoxia and ocean acidification on the inner East China Sea shelf off the Changjiang estuary in August of 2023 during a summer drought. The major reasons of the mitigated hypoxia and ocean acidification are also addressed to get a broader implication.

## 2. Materials and methods

### 2.1. Study area

The East China Sea is located in the temperate northwestern Pacific (Fig. 1). It covers a surface area of 1.25 × 10$^6$ km$^2$, with >70 % of continental shelf shallower than 200 m (Wang et al., 2000). The Changjiang inputs 940 km$^3$ of freshwater (Dai and Trenberth, 2002), 300 × 10$^4$ t of N, 8 × 10$^4$ t of P, and 100 × 10$^4$ t of Si into the East China Sea annually (Gao et al., 2009; Li et al., 2014; Zhang et al., 2007), which reach maximum in summer.

The East China Sea is connected to the Yellow Sea in the north, with a line connecting the northern coast of the Changjiang estuary and the southwestern coast of the Cheju Island separating them (Fig. 1). The climate of the East China Sea is modulated by the East Asian monsoon, with strong northeastern monsoon dominating in winter and relatively weak southwestern monsoon dominating in summer. The Changjiang plume flows northeastward in summer but southwestward along the China mainland coastline in winter (Lee and Chao, 2003). On the northern East China Sea shelf, the Yellow Sea Coastal Current (along the coast of the Jiangsu Province) flows southward year-round, which brings coastal Yellow Sea water characterized by high dissolved inorganic carbon to the coastal East China Sea except in summer under the influence of the strong southwest monsoon (Liu et al., 2021; Yuan et al., 2017). In the offshore area, the northward flowing Kuroshio follows the isobaths beyond the shelf break at ~200 m (Lee and Chao, 2003; Liu et al., 2021). The Kuroshio Current and Changjiang plume mainly dominate mixing on the East China Sea shelf (Yang et al., 2011).

The sea surface temperature (SST) in the East China Sea is low in winter and early spring, but high in summer and early fall (Guo et al., 2015). In addition to the Changjiang input, upwelling of Kuroshio subsurface water is also an important nutrient source on the East China Sea shelf (Chen and Wang, 1999). In general, productivity on the East China Sea shelf is high (primary production up to >1 g C m$^{-2}$ d$^{-1}$) during warm seasons, especially in the Changjiang plume (Gong et al., 2011). In the Changjiang plume, freshwater discharge and biological productivity mainly control the surface water $CO_2$ partial pressure ($pCO_2$) and air-sea $CO_2$ fluxes (Tseng et al., 2014).

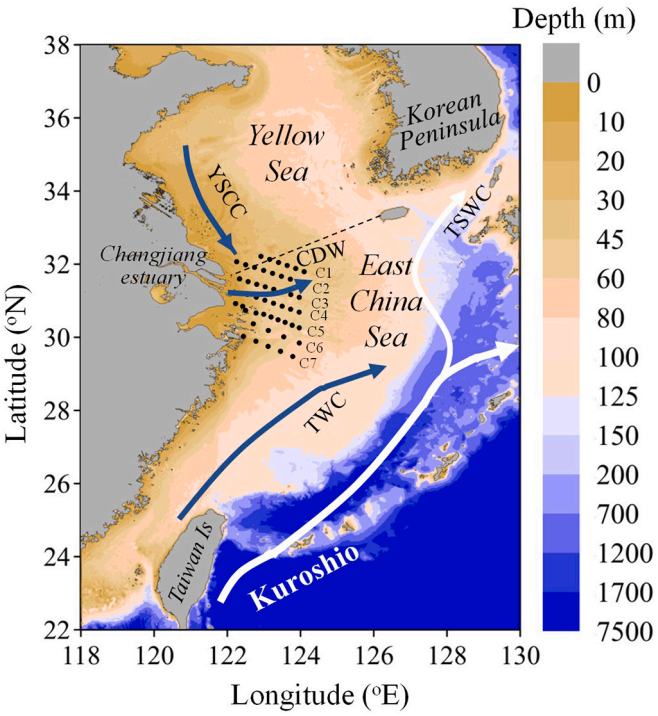


**Fig. 1.** Topographic map of the East China Sea shelf adjacent to the Changjiang estuary with major surface currents in summer. CDW is Changjiang Diluted Water; YSCC is Yellow Sea Coastal Current; TWC is Taiwan Warm Current; TSWC is Tsushima Warm Current. The black dots are the sampling stations and C1–C7 are the names of the transects. (For interpretation of the references to color in this figure legend, the reader is referred to the web version of this article.)

In the productive Changjiang plume in summer, strong stratification occurs with low $pCO_2$ and high dissolved oxygen (DO) in the surface water, versus high $pCO_2$ and low DO in the subsurface and bottom water (Chou et al., 2009). Hypoxia occurs in the bottom water in summer (Li et al., 2002; Wang et al., 2012; Wang et al., 2018; Wei et al., 2007; Zhang et al., 2018; Zhang et al., 2023; Zhu et al., 2017). Strong remineralization of marine-sourced organic matter is the major cause of the summer bottom water hypoxia (Wang et al., 2017; Wang et al., 2016; Wei et al., 2007). Hypoxia in the bottom water is accompanied by enhanced acidification, which is much severe than that induced by the atmospheric $CO_2$ invasion (Cai et al., 2011; Guo et al., 2021).

### 2.2. Sampling and analysis

Seven cross-shelf transects were visited during August 15–22 of 2023 on board R/V Yanping II. At each station, depth profiles of salinity and temperature were measured and recorded with a Seabird® SBE 917 Conductivity-Temperature-Depth/pressure (CTD) sensor package. Discrete water samples were collected at selected depths with 12-L Niskin bottles mounted on a Rosette sampler. Water samples for dissolved oxygen (DO) and carbonate system parameters were collected. Sub-samples for DO, pH, dissolved inorganic carbon (DIC) and total alkalinity (TA) were taken with Tygon® tubing free of air bubbles, with ample sample overflow to minimize contamination from atmospheric oxygen or $CO_2$. Samples for DO were sampled with 60 mL biological oxygen demand bottles and fixed with Winkler regents (Carpenter,

1965). Samples for DIC/pH/TA measurements were taken into 250 mL borosilicate bottles with grounded stoppers and poisoned with 200 μL of saturated $HgCl_2$ solution. The pH/DIC/TA samples were stored in dark at room temperature and returned to the laboratory in Xiamen University for analyses.

All parameters were measured at 25 °C. The samples were placed in a constant-temperature water bath at 25.00 ± 0.01 °C for at least 1 h before measurements. DO samples were measured spectrophotometrically at 466 nm on onboard within 4 h of sampling (Labasque et al., 2004). pH and DIC were measured simultaneously, and TA values were measured within two days after the DIC and pH measurements. DIC values were measured with a DIC Analyzer (Apollo SciTech model AS-C6L) with a precision of better than ±2 μmol $kg^{-1}$. pH values were measured spectrophotometrically with a home-made automatic system integrated with an Agilent 8453 spectrophotometer with a precision of ±0.0005 and the measured pH values were in total hydrogen scale at 25 °C (Dickson et al., 2007). TA values were determined with a Gran titration method using an automated alkalinity titrator (Apollo SciTech model AS-ALK3) with a precision of better than ±2 μmol $kg^{-1}$. Both DIC and TA measurements were calibrated with the certified reference material (CRM) provided by Dr. Andrew Dickson of the Scripps Institution of Oceanography to achieve an accuracy better than ±2 μmol $kg^{-1}$.

### 2.3. Data processing

As pH values were sensitive to temperature, two sets of values were presented in this study. pH values at 25 °C and at in situ temperatures were indicted by $pH_{25}$ and $pH_{in\text{-}situ}$, respectively. $pH_{25}$ were the measured values, while $pH_{in\text{-}situ}$ were calculated with the program CO2SYS (version 14) (Pierrot et al., 2006) with DIC and TA as input parameters. The dissolution constants of carbonic acid were from Millero et al. (2006). The $CO_2$ solubility coefficient was from Weiss (1974) and sulfate dissociation constant was from Dickson (1990). Saturation state index of aragonite ($\Omega_{Ar}$) was also calculated with the program CO2SYS (version 14) (Pierrot et al., 2006) and the parameters input and coefficient selections were the same with the calculations of $pH_{in\text{-}situ}$.

The DIC and $pH_{25}$ values at $CO_2$ equilibrium with the atmosphere ($DIC_{Equ.}$ and $pH_{25,\ Equ.}$) were calculated with TA and atmospheric $pCO_2$ with the program CO2SYS (version 14) (Pierrot et al., 2006), and the parameters input and coefficient selections were the same with the calculations of $pH_{in\text{-}situ}$ and $\Omega_{Ar}$. The measured average atmospheric $pCO_2$ during the cruise (410 μatm) was taken.

Excess DIC was defined as the difference between the observed DIC and $DIC_{Equ}$ following Xu et al. (2017). Similarly, the $pH_{25}$ and $\Omega_{Ar}$ changes due to organic matter remineralization were defined as the differences between the observed values and the values at equilibrium

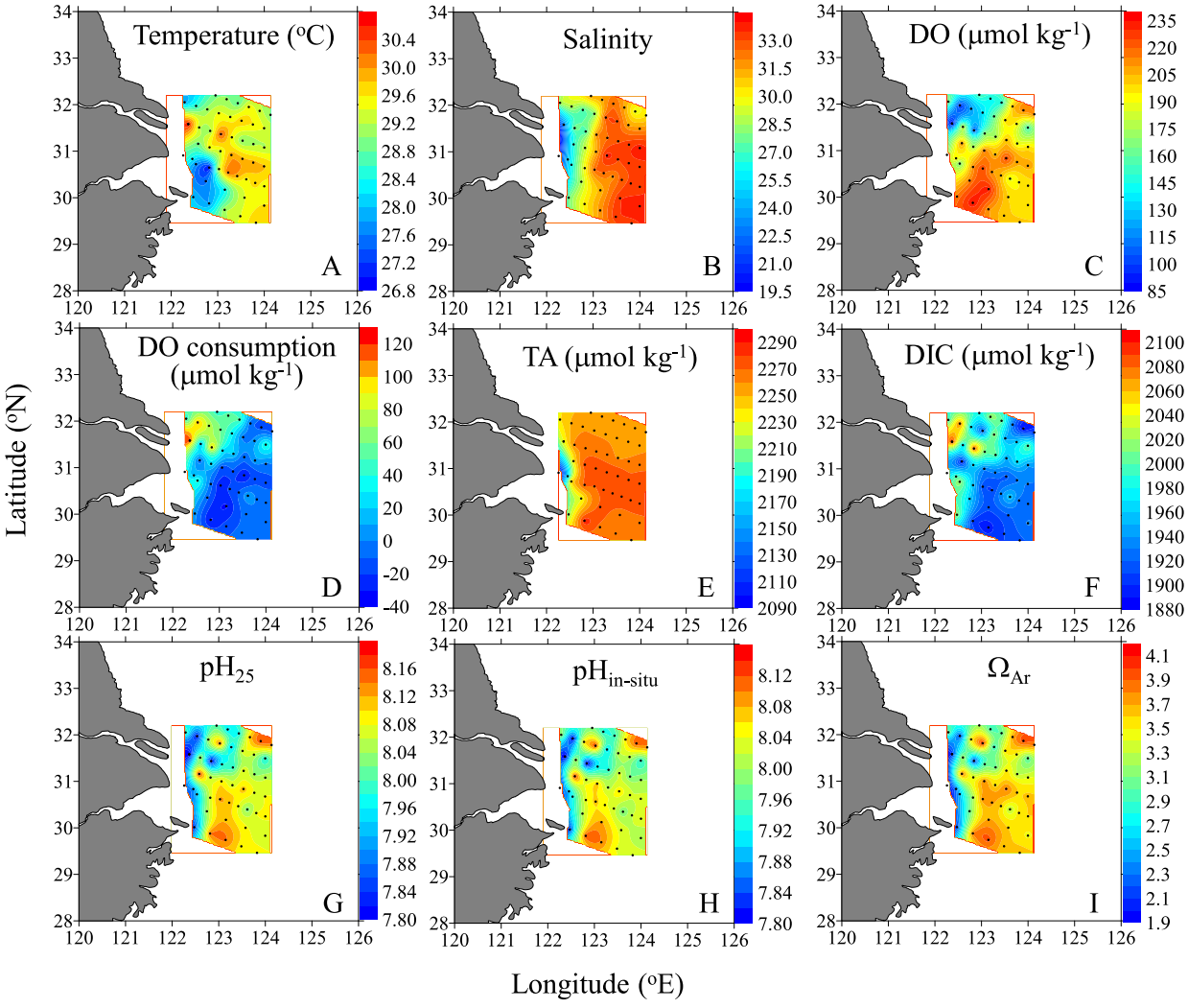


**Fig. 2.** Temperature, salinity, dissolved oxygen (DO), DO consumption, total alkalinity (TA), dissolved inorganic carbon (DIC), pH at 25 °C ($pH_{25}$), pH at in situ temperature ($pH_{in\text{-}situ}$) and saturation state index of aragonite ($\Omega_{Ar}$) in the surface water of the East China Sea shelf in August of 2023. The black dotes are the sampling stations.

with the atmosphere (Guo et al., 2023). DO consumption is defined as the difference between the saturated DO and the observed DO, the former of which was calculated according to the empirical formula of Benson and Krause (1984).

The satellite chlorophyll data were retrieved from the MODIS (Moderate Resolution Imaging Spectroradiometer) onboard the NASA Aqua satellite. Level-3 standard mapped image of 4 km resolution chlorophyll in August of 2023, and 2009, 2013 and 2016 (as references) were obtained from the Asia-Pacific Data Research Center (http://apdrc.soest.hawaii.edu:80/dods/public_data/satellite_product/MODIS_Aqua/chla_mapped_mon_4km).

## 3. Results

### 3.1. Hydrological settings

Surface water temperature ranged 27.0–30.6 °C (29.2 ± 0.7 °C), and the spatial distribution was patchy (Fig. 2A). Low temperature was at the southwestern corner of the study area, and high temperature was at the Changjiang estuary mouth and the center of the study area. Surface water salinity ranged 20.4–33.9 (30.7 ± 3.0), with low values at the inshore zone and increased offshore (Fig. 2B).

In the bottom water, temperature ranged 19.0–28.4 °C (21.9 ± 2.3 °C), with highest temperatures located at the inshore zone and low temperatures at the southeastern zone (Fig. 3A). This was mainly attributed to the influence of the high-temperature river water. Salinity ranged 20.9–34.5 (33.1 ± 2.4). Low salinities were observed in the inshore and the northern zones which were attributed to the river water dilution and the influence of the Yellow Sea water. High salinities were observed in the open East China Sea (Fig. 3B).

### 3.2. Spatial distributions of DO and carbonate parameters

#### 3.2.1. Surface water

In the surface water, DO ranged 87.3–234.5 μmol $kg^{-1}$ (39.1 %–116.6 %). Low DO was near the Changjiang estuary and the northwestern corner of the study area (Fig. 2C). Spatial distribution of DO consumption was opposite to that of DO, and DO consumption ranged −32.2 to 116.3 μmol $kg^{-1}$. There was DO production (negative DO consumption values) in the southeastern zone. However, in the inshore zone and the northwestern corner of the study area, there was high DO consumption (>100 μmol $kg^{-1}$) (Fig. 2D).

Generally, the spatial distribution pattern of TA followed that of salinity, i.e. lowest TA (<2100 μmol $kg^{-1}$) was in the inshore zone, and high values (>2250 μmol $kg^{-1}$) were in the open East China Sea (Fig. 2E). Different from the TA distribution pattern, spatial distribution

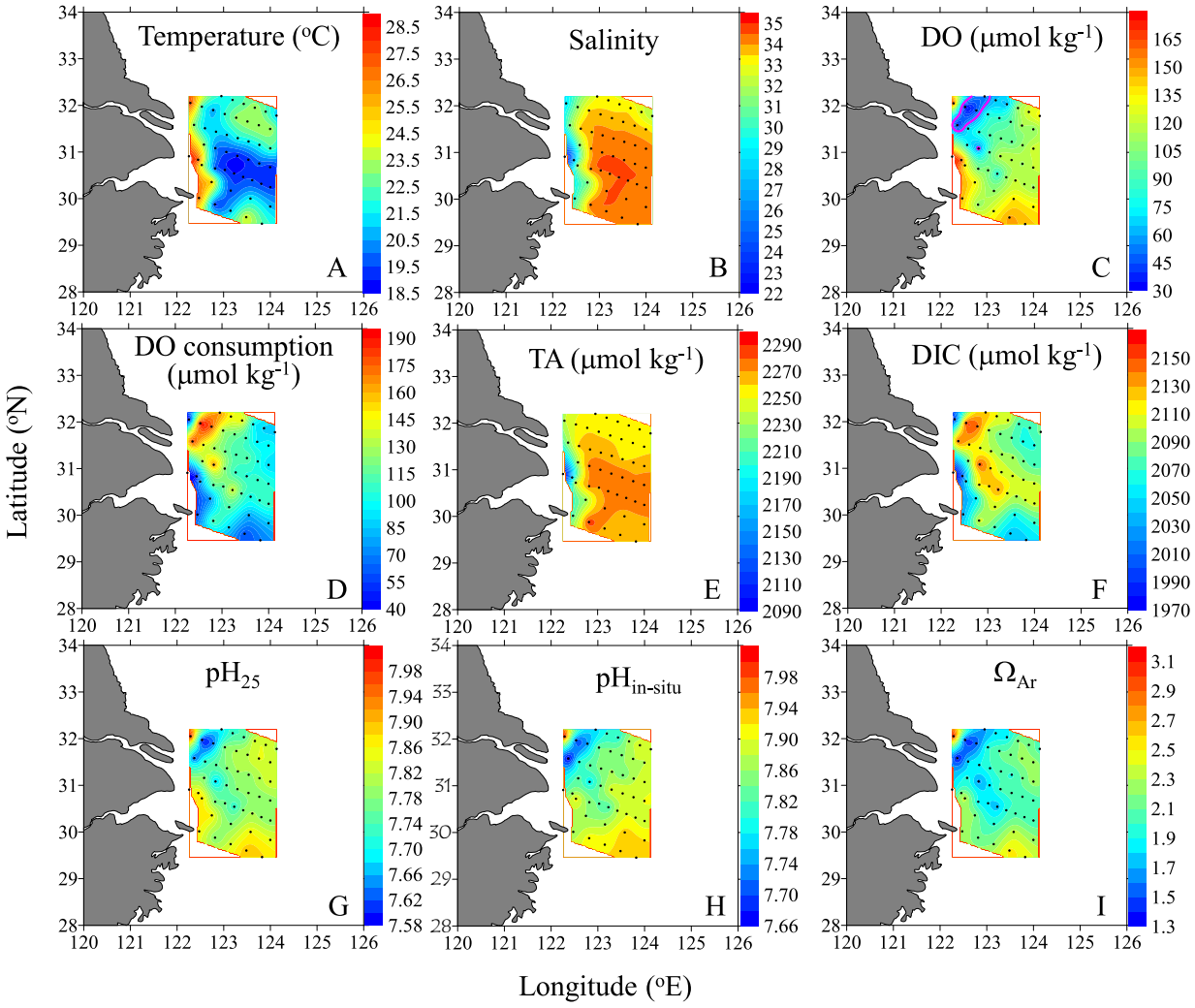


**Fig. 3.** Temperature, salinity, dissolved oxygen (DO), DO consumption, total alkalinity (TA), dissolved inorganic carbon (DIC), pH at 25 °C ($pH_{25}$), pH at in situ temperature ($pH_{in\text{-}situ}$) and saturation state index of aragonite ($\Omega_{Ar}$) in the bottom water of the East China Sea shelf in August of 2023. The black dotes are the sampling stations. The area enclosed by magenta curve is the hypoxic zone. (For interpretation of the references to color in this figure legend, the reader is referred to the web version of this article.)

of DIC was patchy. There were two patches of highest DIC (>2050 μmol $kg^{-1}$) near the Changjiang estuary. However, DIC in the southwestern zone was lowest (<1950 μmol $kg^{-1}$) although salinity was high (Fig. 2F).

Spatial distributions of pH were also patchy and generally opposite to that of DIC. $pH_{25}$ and $pH_{in\text{-}situ}$ range were 7.80–8.17 and 7.79–8.13, respectively (Fig. 2G and H). The $pH_{in\text{-}situ}$ values were lower than $pH_{25}$ due to the fact that $pH_{in\text{-}situ}$ decreases with temperature. As temperature in the entire study area was higher than 25 °C, $pH_{in\text{-}situ}$ was lower than $pH_{25}$. High pH values were in the southeastern zone where DIC was low; lowest pH values were in the inshore zone and the high-DIC patches (Fig. 2G and H). $\Omega_{Ar}$ ranged 1.89–4.05, and the distribution pattern was similar to those of pH, i.e. with lowest values in the inshore zone and the high-DIC patches and high values in the southeastern zone (Fig. 2I).

#### 3.2.2. Bottom water

In the bottom water, DO ranged 32.0–171.6 μmol $kg^{-1}$ (14 %–80 %). There was two patches of low DO in the inshore zone. If DO <63 μmol $kg^{-1}$ (2 mg $L^{-1}$) is defined as hypoxia, only the northwestern corner and a station in the C4 section was hypoxic (5 stations totally, enclosed by the magenta curves in Fig. 3C). The area of the hypoxic zone was ~2000 $km^2$. DO consumption ranged 41.8–189.8 μmol $kg^{-1}$ and its spatial distribution pattern was opposite to that of DO (Fig. 3D).

Spatial distribution of TA was also similar to that of salinity, i.e. low TA values (<2100 μmol $kg^{-1}$) at the Changjiang estuary and high TA values (>2250 μmol $kg^{-1}$) in the open East China Sea (Fig. 3E). DIC distribution in bottom water was patchy, and there were two high-DIC patches (>2130 μmol $kg^{-1}$) off the Changjiang estuary. However, DIC in the inshore low-salinity zone was low, which might be influenced by the Changjiang freshwater input (Fig. 3F). Spatial distributions of both $pH_{25}$ and $pH_{in\text{-}situ}$ were opposite to that of DIC. $pH_{25}$ and $pH_{in\text{-}situ}$ ranged 7.63–8.04 and 7.66–8.00, respectively (Fig. 3G and H). $\Omega_{Ar}$ ranged 1.34–3.06, and the spatial distribution pattern was similar to that of pH, and opposite to that of DIC (Fig. 3I). The spatial distribution of DIC was opposite to that of DO, and the spatial distribution pattern of pH was similar to that of DO, suggesting the domination of strong remineralization of organic matter.

## 4. Discussion

### 4.1. DIC consumption in surface water and addition in bottom water

Surface water of the southeastern zone was characterized by low DIC, high pH, high $\Omega_{Ar}$ and high DO and negative DO consumption (DO production), which suggests net biological uptake of DIC and production of DO. Conversely, the surface water off the Changjiang estuary and the northwestern zone was characterized by high DIC, low pH, low $\Omega_{Ar}$, low DO and conspicuous DO consumption, which might be influenced by the upwelled bottom water as shown by the vertical distributions (Fig. S2). The high DIC, low pH and low DO in the inshore surface water were also observed in August of 2016 (Guo et al., 2021), which suggest that this phenomenon might be common in summer.

Comparison of the observed DIC and DO with the $DIC_{Equ.}$ and DO saturation showed that DIC was lower than the $DIC_{Equ}$ (Fig. 4A)., while DO was higher than the DO saturation (Fig. 4B) in the surface water of the southeastern zone. Average DIC removal was 8.9 ± 20.4 μmol $kg^{-1}$, and average DO production was 13.1 ± 10.2 μmol $kg^{-1}$. However, in the surface water of the northwestern zone, DIC was higher than the $DIC_{Equ}$ (Fig. 4A) and DO was lower than DO saturation (Fig. 4B).

In the bottom water, DIC in the entire study area was higher than the $DIC_{Equ.}$ (Fig. 4C), while DO was lower than the DO saturation (Fig. 4D). The average DIC addition and DO consumption were 84.1 ± 24.3 μmol $kg^{-1}$ and 100.8 ± 33.6 μmol $kg^{-1}$, respectively. The ratio of DIC addition to DO consumption was 0.77, which was the same with the Redfield ratio (Redfield et al., 1963). This suggests that the DIC addition and the DO consumption was mainly attributed to the remineralization of eutrophication induced marine-sourced organic matter (Wang et al., 2017; Wang et al., 2020).

Compared with previous observations, the DIC removal (8.9 ± 20.4 μmol $kg^{-1}$) in the surface water in August of 2023 was much lower than that in August of 2009 and 2013 (88 μmol $kg^{-1}$) (Wang et al., 2017), and August of 2016 (90 μmol $kg^{-1}$) (Yao, 2019).

The nutrients input fluxes from the Changjiang was dominated by river discharge (Gao et al., 2012; Wang et al., 2019). Model results suggest that chlorophyll concentration on the East China Sea shelf off the Changjiang estuary was dominated by the Changjiang nutrient supply (Xu et al., 2020a). Liu et al. (2015) also report the relationship

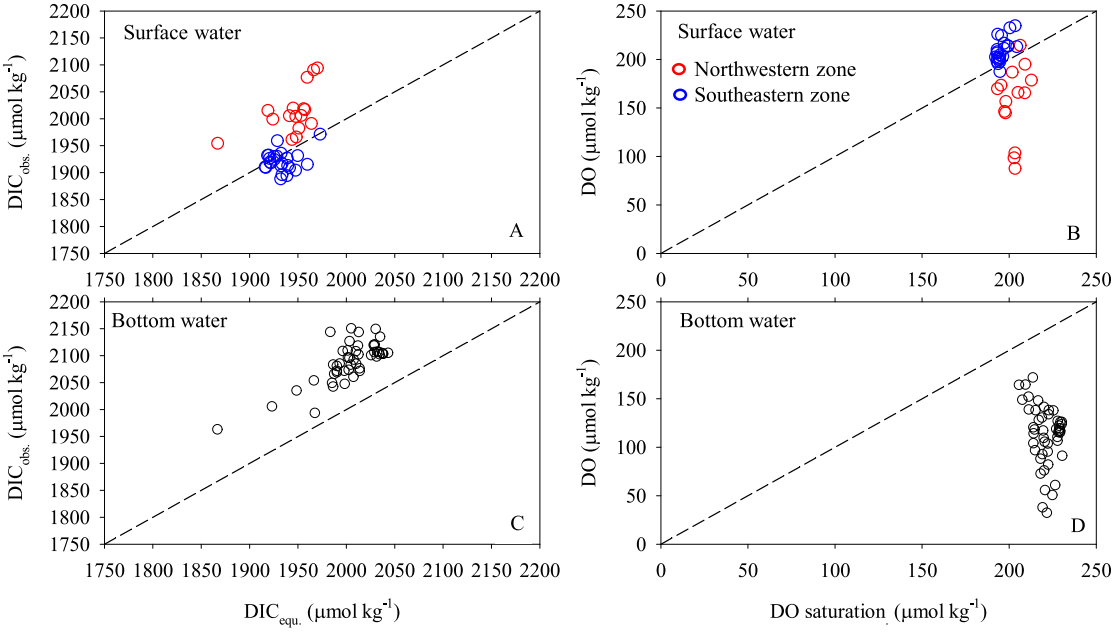


**Fig. 4.** Relationship of observed DIC ($DIC_{obs.}$) and DIC at equilibrium with the atmosphere ($DIC_{equ.}$), and observed DO with the DO saturation in surface and bottom waters. The dashed lines are the 1:1 lines.

between the primary production and the Changjiang nutrient discharge. This is consistent with the field observations. Gong et al. (2011) found that the Changjiang flood is the major regulator of the phytoplankton biomass on the East China Sea shelf. Therefore, the low freshwater discharge from the Changjiang in the summer of 2023 would result in low phytoplankton biomass. In fact, the satellite derived chlorophyll concentration in the surveyed area (29.25–32.5 N, 122–124.25°E) in August of 2023 (2.26 μg $L^{-1}$) were much lower than those in August of 2009 (4.48 μg $L^{-1}$), 2013 (3.51 μg $L^{-1}$) and 2016 (3.74 μg $L^{-1}$) (Fig. 5) or the monthly average from 2004 to 2022 (3.79 μg $L^{-1}$).

As a consequence of the low phytoplankton biomass in the surface water, the amount of the settling and the subsequent remineralization of the marine-sourced organic matter would be also lower. Chen et al. (2009) reported the domination of the Changjiang discharge on the community respiration on the East China Sea shelf. Liu et al. (2015) also report the Changjiang discharge dominating the seafloor DO demand. The field measured DIC addition in the bottom water in August of 2023 (84.1 ± 24.3 μmol $kg^{-1}$) was much lower than that in August of 2016 (145 μmol $kg^{-1}$). The lowered amount of the organic matter remineralization in August of 2023 mitigated the status of hypoxia and ocean acidification, which will be discussed in the next section.

### 4.2. Mitigation of hypoxia and acidification in the bottom water impacted by the summer drought

In August of 2023, average DO in the bottom water was 112.4 ± 31.1 μmol $kg^{-1}$, and the lowest DO was 32.0 μmol $kg^{-1}$. The lowest DO was slightly higher than or similar to those in other summer after 2000 (Wang et al., 2021; Zhu et al., 2017), and much higher than that in August of 2016 (3.3 μmol $kg^{-1}$) (Table 1, Guo et al., 2021). The hypoxic area off the Changjiang estuary usually ranges from >5000 to 20,000 $km^2$ after the year 2000 (Wang et al., 2021; Zhu et al., 2017). Hypoxic area in August of 2016 was ~11,000 $km^2$ (Table 1; Yao, 2019). However, the hypoxic area in August of 2023 was only ~2000 $km^2$. Compared to the literature reports, the hypoxic area in August of 2023 was much smaller, and the minimum DO concentration was higher than other summer.

**Table 1**
Comparison of bottom hypoxia and acidification in August of 2023 with 2016.

| Parameter | August 2023 | August of 2016[a] |
|---|---|---|
| Average DO (μmol $kg^{-1}$) | 112.4 ± 31.1 | 85.5 ± 38.9 |
| Minimum DO (μmol $kg^{-1}$) | 32.0 | 3.3 |
| DO consumption (μmol $kg^{-1}$) | 108.8 ± 33.6 | 138.8 ± 39.9 |
| Hypoxic area ($km^2$) | 2000 | 11,000 |
| $pH_{25}$ | 7.814 ± 0.069 | 7.801 ± 0.084 |
| Minimum $pH_{25}$ | 7.629 | 7.601 |
| $\Omega_{Ar}$ | 2.03 ± 0.28 | 1.98 ± 0.34 |
| Minimum $\Omega_{Ar}$ | 1.34 | 1.27 |
| pH decrease | 0.179 ± 0.061 | 0.205 ± 0.086 |
| $\Omega_{Ar}$ decrease | 0.82 ± 0.23 | 0.87 ± 0.32 |

[a] From Guo et al. (2021).

Excess DIC increases with DO consumption (Fig. 6A), and the ratio of DIC addition to DO consumption was 0.77 as stated above. This ratio is very consistent with that in August of 2016 (0.75) (Guo et al., 2021). Additionally, $pH_{25}$ decrease with Excess DIC (Fig. 6B). Similar to pH, $\Omega_{Ar}$ also decreases with Excess DIC, which was due to the fact that $\Omega_{Ar}$ was dominated by pH (Zeebe and Wolf-Gladrow, 2003). $\Delta pH_{25}$ and $\Delta\Omega_{Ar}$ also decreased with the Excess DIC linearly (Fig. 6C), suggesting the domination of the organic matter remineralization influence (Fig. 6D and E). $\Delta pH_{25}$ and $\Delta\Omega_{Ar}$ ranged −0.05 to −0.38 and −0.28 to −1.53, respectively. Averaged the entire study area, $pH_{25}$ and $\Omega_{Ar}$ decreases were 0.179 ± 0.061 and 0.82 ± 0.23, respectively, in the bottom water in August of 2023 (Table 1).

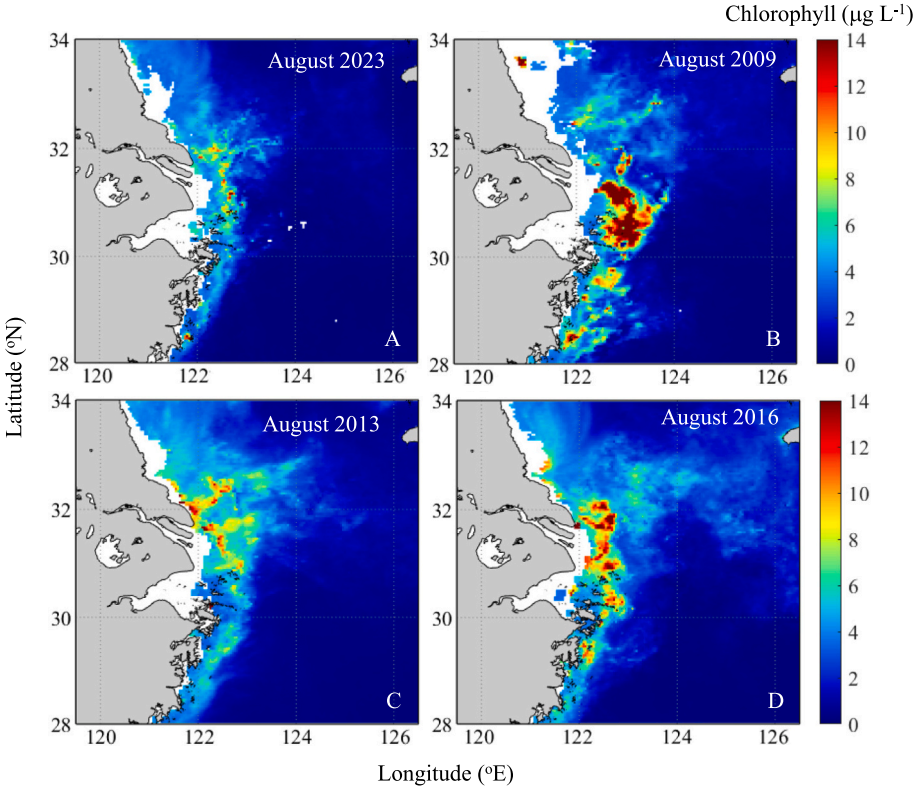


**Fig. 5.** Spatial distribution of monthly average satellite derived chlorophyll concentration in August of 2023 (A), and August of 2009 (B), 2013 (C) and 2016 (D) on the East China Sea shelf. The data are MODIS-Aqua level-3 standard mapped image of 4 km chlorophyll concentration, which were obtained from the Asia-Pacific Data Research Center (http://apdrc.soest.hawaii.edu:80/dods/public_data/satellite_product/MODIS_Aqua/chla_mapped_mon_4km). (For interpretation of the references to color in this figure legend, the reader is referred to the web version of this article.)

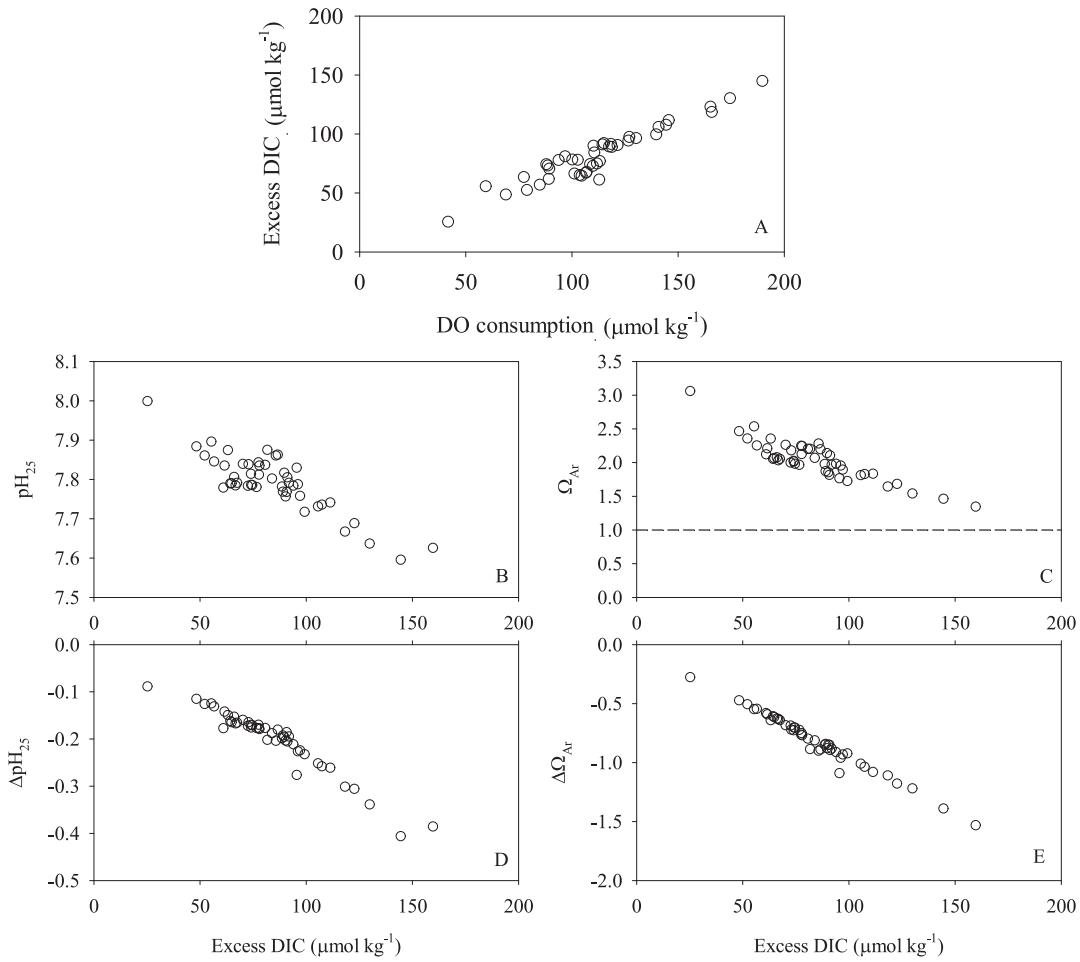


**Fig. 6.** Relationship of excess DIC with DO consumption (A), and pH at 25 °C (pH $_{25}$, B), $\Omega_{Ar}$ (C), $pH_{25}$ change ($\Delta pH_{25}$, D) and $\Omega_{Ar}$ change ($\Delta\Omega_{Ar}$, E) resulted from organic matter remineralization with excess DIC in the bottom water. Dashed line in panel C shows $\Omega_{Ar} = 1$.

$pH_{25}$ range of the bottom water of August of 2023 was 7.814 ± 0.069 and the minimum value was 7.629. Both the average and the minimum values were higher than those of 2016 (Table 1). The average and minimum $\Omega_{Ar}$ values in the bottom water of August of 2023 were 2.03 ± 0.28 and 1.34, respectively, which were also higher than those in 2016 (Table 1). The largest $pH_{25}$ and $\Omega_{Ar}$ decrease in the bottom water of August of 2023 were 0.38 and 1.53, respectively, and they were located in the northwestern zone (the hypoxic zone). The $\Omega_{Ar}$ in the hypoxic zone in August of 2023 were 1.34–1.68, which were higher than in August of 2016 (1.31–1.60, Guo et al., 2021) and 2017 (1.21–1.29, Xiong et al., 2020). That is to say, as a consequence of the decreased organic matter remineralization, acidification in August of 2023 also mitigated.

Additionally, weakened water stratification on the shelf due to the decreased freshwater discharge might also play a role in mitigating bottom water hypoxia and acidification (Zhao et al., 2020). On the East China Sea shelf, the Changjiang plume played a significant role in controlling the stratification (Zhang et al., 2019). Decreasing river discharge reduces the water stratification and thereby increases the vertical oxygen supply from the surface water (Zheng et al., 2016). Continuous monitoring shows that the DO variation in the bottom water is closely related to that of water stratification (Ni et al., 2016). Model results show that the bottom DO response to the stratification at only 6–50 h (Zhang et al., 2018). Therefore, decreased freshwater discharge in the summer of 2023 might weaken the water stratification, which might also mitigate hypoxia and acidification of the bottom water.

To sum up, DO, pH and $\Omega_{Ar}$ values in the bottom water increased, and hypoxic area shrunk as a result of lowered remineralization of organic matter in August of 2023 compared to the previous summer. The drought in the summer of 2023 decreased the organic carbon production in the surface water and subsequently the remineralization in the bottom water and sediment on the East China Sea shelf. The lower organic matter remineralization mitigated hypoxia and acidification. The weakened water stratification as a result of the decreased freshwater discharge might also play a role. These processes can be represented by the schematic diagram of Fig. 7.

Although hypoxia and acidification in August of 2023 was mitigated compared to the other summer conditions, $pH_{25}$ and $\Omega_{Ar}$ decrease were still conspicuous. The lowest $pH_{25}$ and $\Omega_{Ar}$ were 7.63 and 1.34, respectively. $\Omega_{Ar}$ value of 1.5 was regarded as a critical threshold for marine shellfish development (Ekstrom et al., 2015; Waldbusser et al., 2015). Although acidification in August of 2023 was mitigated, the $\Omega_{Ar}$ values in the hypoxic zone were still below the threshold value of 1.5. Regulating the anthropogenic influence on the river water quality and the marginal seas are still urgently needed to mitigate the acidification status.

## 5. Concluding remarks

This study reports a field observed mitigation of hypoxia and acidification in a dry summer on the East China Sea shelf, a well-known summer hypoxic zone. The freshwater discharge from the Changjiang in the three months in the summer of 2023 was only ~60 % of the long-term monthly average. As a consequence, chlorophyll concentration on the East China Sea shelf was conspicuously lowered (2.26 μg $L^{-1}$ in August of 2023 as compared to 3.79 μg $L^{-1}$, the monthly average from

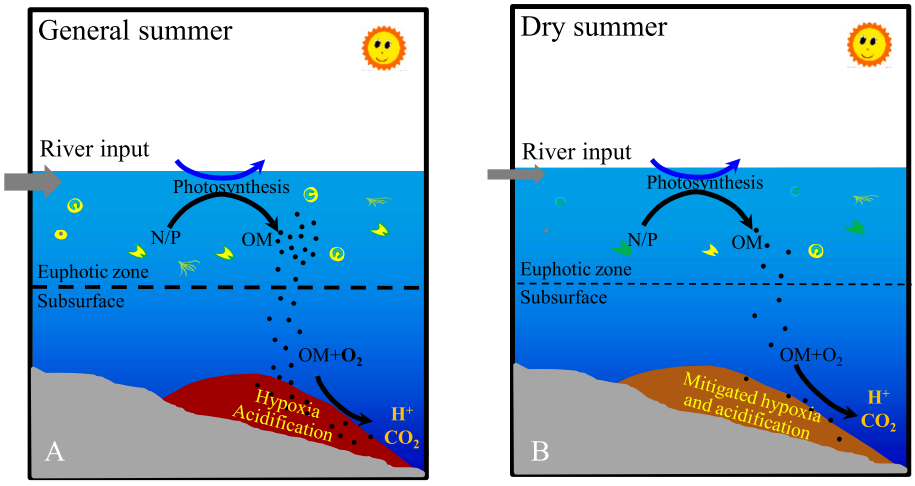


**Fig. 7.** Conceptual model of the mitigation of hypoxia and acidification in the bottom water on the ECS shelf. N/P indicates nutrients and OM is organic matter. The dashed lines represent the bottom of the euphotic zone; the thin dashed lines in panel B represent the weakened stratification.

2004 to 2022). Filed observations found that DO consumption and the DIC addition in the bottom water were decreased due to the lowered remineralization of organic matter and weakened stratification. Consequently, hypoxia and acidification in the bottom water were mitigated. This suggests that decrease in river discharge may mitigate hypoxia and acidification in the adjacent coastal waters. However, as a large river, the influence of the Changjiang on the acidification of the bottom water on the East China Sea shelf is still very severe even during a drought. Regulating the anthropogenic impact on the river water quality and subsequently the coastal marginal seas are still urgently needed to mitigate the acidification status.

## CRediT authorship contribution statement

**Shiping Lei:** Writing – original draft, Investigation, Conceptualization. **Dezhi Bu:** Writing – review & editing, Methodology, Conceptualization. **Xianghui Guo:** Writing – review & editing, Methodology, Formal analysis, Conceptualization. **Yi Xu:** Writing – review & editing, Investigation, Data curation. **Yi Yang:** Writing – review & editing, Investigation, Data curation. **Shuqi An:** Writing – review & editing, Investigation, Conceptualization. **Yan Li:** Writing – review & editing, Data curation. **Jinyan Pang:** Writing – review & editing, Data curation. **Kuanbo Zhou:** Writing – review & editing, Funding acquisition.

## Declaration of competing interest

The authors declare that the study was conducted in the absence of any commercial or financial relationships that could be construed as potential conflicts of interest.

## Data availability

Data are available from the corresponding author.

## Acknowledgements

Zhaozhang Chen and Longqi Yang organized the CTD sampling and processed the CTD data. We thank the crews of R/V Yanping II for their assistance during the cruise. Chief scientist Dr. Jinyu Yang was appreciated for the help during the cruise. The study was supported by the National Key Research and Development Projects (2022YFC3105302), the Strategic Priority Research Program of Chinese Academy of Sciences (XDB42000000) and the Natural Science Foundation of China (42141001).

## Appendix A. Supplementary data

Supplementary data to this article can be found online at https://doi.org/10.1016/j.marpolbul.2024.116830.

## References

Benson, B.B., Krause, D., 1984. The concentration and isotopic fractionation of oxygen dissolved in freshwater and seawater in equilibrium with the atmosphere. Limnol. Oceanogr. 29 (3), 620–632. https://doi.org/10.4319/lo.1984.29.3.0620.

Caballero-Alfonso, A.M., Carstensen, J., Conley, D.J., 2015. Biogeochemical and environmental drivers of coastal hypoxia. J. Mar. Syst. 141, 190–199. https://doi.org/10.1016/j.jmarsys.2014.04.008.

Cai, W.-J., Hu, X., Huang, W.-J., Murrell, M.C., Lehrter, J.C., Lohrenz, S.E., Chou, W.-C., Zhai, W., Hollibaugh, J.T., Wang, Y., Zhao, P., Guo, X., Gundersen, K., Dai, M., Gong, G.-C., 2011. Acidification of subsurface coastal waters enhanced by eutrophication. Nat. Geosci. 4 (11), 766–770. https://doi.org/10.1038/ngeo1297.

Carpenter, J.H., 1965. The Chesapeake Bay Institute technique for the Winkler dissolved oxygen method. Limnol. Oceanogr. 10, 141–143. https://doi.org/10.4319/lo.1965.10.1.0141.

Carstensen, J., Andersen, J.H., Gustafsson, B.G., Conley, D.J., 2014. Deoxygenation of the Baltic Sea during the last century. Proc. Natl. Acad. Sci. U. S. A. 111 (15), 5628–5633. https://doi.org/10.1073/pnas.1323156111.

Chen, C.T.A., Wang, S.L., 1999. Carbon, alkalinity and nutrient budgets on the East China Sea continental shelf. J. Geophys. Res. 104 (C9), 20675–20686. https://doi.org/10.1029/1999jc900055.

Chen, C.C., Shiah, F.K., Chiang, K.P., Gong, G.C., Kemp, W.M., 2009. Effects of the Changjiang (Yangtze) River discharge on planktonic community respiration in the East China Sea. J. Geophys. Res. Oceans 114, C03005. https://doi.org/10.1029/2008jc004891.

Chou, W.C., Gong, G.C., Sheu, D.D., Jan, S., Hung, C.C., Chen, C.C., 2009. Reconciling the paradox that the heterotrophic waters of the East China Sea shelf act as a significant $CO_2$ sink during the summertime: evidence and implications. Geophys. Res. Lett. 36, L15607 https://doi.org/10.1029/2009gl038475.

Chou, W.C., Gong, G.C., Hung, C.C., Wu, Y.H., 2013. Carbonate mineral saturation states in the East China Sea: present conditions and future scenarios. Biogeosciences 10 (10), 6453–6467. https://doi.org/10.5194/bg-10-6453-2013.

Dai, A., Trenberth, K.E., 2002. Estimates of freshwater discharge from continents: Latitudinal and seasonal variations. J. Hydrometeorol. 3 (6), 660–687. https://doi.org/10.1175/1525-7541(2002)003<0660:eofdfc>2.0.co;2.

Dickson, A.G., 1990. Standard potential of the reaction AgCl (S)+1/2H2(G)=Ag (S)+HCl (Aq), and the standard acidity constant of the ion HSO4- in synthetic seawater from 273.15K to 318.15K. J. Chem. Thermodyn. 22 (2), 113–127. https://doi.org/10.1016/0021-9614(90)90074-z.

Dickson, A.G., Sabine, C.L., Christian, J.R., 2007. Guide to Best Practices for Ocean $CO_2$ Measurement, 191 pp.. PICES Special Publication 3.

Ekstrom, J.A., Suatoni, L., Cooley, S.R., Pendleton, L.H., Waldbusser, G.G., Cinner, J.E., Ritter, J., Langdon, C., van Hooidonk, R., Gledhill, D., Wellman, K., Beck, M.W., Brander, L.M., Rittschof, D., Doherty, C., Edwards, P.E.T., Portela, R., 2015. Vulnerability and adaptation of US shellfisheries to ocean acidification. Nat. Clim. Chang. 5 (3), 207–214. https://doi.org/10.1038/nclimate2508.

Feely, R.A., Alin, S.R., Newton, J., Sabine, C.L., Warner, M., Devol, A., Krembs, C., Maloy, C., 2010. The combined effects of ocean acidification, mixing, and respiration on pH and carbonate saturation in an urbanized estuary. Estuar. Coast. Shelf Sci. 88 (4), 442–449. https://doi.org/10.1016/j.ecss.2010.05.004.

Feely, R.A., Okazaki, R.R., Cai, W.-J., Bednarsek, N., Alin, S.R., Byrne, R.H., Fassbender, A., 2018. The combined effects of acidification and hypoxia on pH and aragonite saturation in the coastal waters of the California current ecosystem and the northern Gulf of Mexico. Cont. Shelf Res. 152, 50–60. https://doi.org/10.1016/j.csr.2017.11.002.

Fennel, K., Testa, J.M., 2019. Biogeochemical controls on coastal hypoxia. In: Carlson, C. A., Giovannoni, S.J. (Eds.), Annual Review of Marine Science, vol 11, pp. 105–130. https://doi.org/10.1146/annurev-marine-010318-095138.

Gao, L., Li, D.-J., Ding, P.-X., 2009. Quasi-simultaneous observation of currents, salinity and nutrients in the Changjiang (Yangtze River) plume on the tidal timescale. J. Mar. Syst. 75 (1–2), 265–279. https://doi.org/10.1016/j.jmarsys.2008.10.006.

Gao, L., Li, D., Zhang, Y., 2012. Nutrients and particulate organic matter discharged by the Changjiang (Yangtze River): seasonal variations and temporal trends. J. Geophys. Res.-Biogeosci. 117, G04001 https://doi.org/10.1029/2012jg001952.

Gong, G.-C., Liu, K.-K., Chiang, K.-P., Hsiung, T.-M., Chang, J., Chen, C.-C., Hung, C.-C., Chou, W.-C., Chung, C.-C., Chen, H.-Y., Shiah, F.-K., Tsai, A.-Y., Hsieh, C.-H., Shiao, J.-C., Tseng, C.-M., Hsu, S.-C., Lee, H.-J., Lee, M.-A., Lin, I.I., Tsai, F., 2011. Yangtze River floods enhance coastal ocean phytoplankton biomass and potential fish production. Geophys. Res. Lett. 38, L13603 https://doi.org/10.1029/2011gl047519.

Grantham, B.A., Chan, F., Nielsen, K.J., Fox, D.S., Barth, J.A., Huyer, A., Lubchenco, J., Menge, B.A., 2004. Upwelling-driven nearshore hypoxia signals ecosystem and oceanographic changes in the northeast Pacific. Nature 429 (6993), 749–754. https://doi.org/10.1038/nature02605.

Guo, X.H., Zhai, W.D., Dai, M.H., Zhang, C., Bai, Y., Xu, Y., Li, Q., Wang, G.Z., 2015. Air-sea $CO_2$ fluxes in the East China Sea based on multiple-year underway observations. Biogeosciences 12 (18), 5495–5514. https://doi.org/10.5194/bg-12-5495-2015.

Guo, X.H., Yao, Z.T., Gao, Y., Luo, Y.H., Xu, Y., Zhai, W.D., 2021. Seasonal variability and future projection of ocean acidification on the East China Sea shelf off the Changjiang estuary. Front. Mar. Sci. 8 https://doi.org/10.3389/fmars.2021.770034.

Guo, X., Su, J., Guo, L., Liu, Z., Yang, W., Li, Y., Yao, Z., Wang, L., Dai, M., 2023. Coupling of carbon and oxygen in the Pearl River plume in summer: upwelling, hypoxia, reoxygenation and enhanced acidification. J. Geophys. Res. Oceans 128 (8), 2022JC019326. https://doi.org/10.1029/2022jc019326.

Jiang, Z.-P., Cai, W.-J., Chen, B., Wang, K., Han, C., Roberts, B.J., Hussain, N., Li, Q., 2019. Physical and biogeochemical controls on pH dynamics in the northern Gulf of Mexico during summer hypoxia. J. Geophys. Res. Oceans 124 (8), 5979–5998. https://doi.org/10.1029/2019jc015140.

Jutras, M., Dufour, C.O., Mucci, A., Cyr, F., Gilbert, D., 2020. Temporal changes in the causes of the observed oxygen decline in the St. Lawrence estuary. J. Geophys. Res. Oceans 125 (12). https://doi.org/10.1029/2020jc016577.

Labasque, T., Chaumery, C., Aminot, A., Kergoat, G., 2004. Spectrophotometric winkler determination of dissolved oxygen: re-examination of critical factors and reliability. Mar. Chem. 88 (1–2), 53–60. https://doi.org/10.1016/j.marchem.2004.03.004.

Lee, H.J., Chao, S.Y., 2003. A climatological description of circulation in and around the East China Sea. Deep-Sea Res. II 50 (6–7), 1065–1084. https://doi.org/10.1016/s0967-0645(03)00010-9.

Li, D., Zhang, J., Huang, D., Wu, Y., Liang, J., 2002. Oxygen depletion off the Changjiang (Yangtze River) Estuary. Sci. China. Ser. D Earth Sci. 45 (12), 1137–1146. https://doi.org/10.1360/02yd9110.

Li, H.-M., Tang, H.-J., Shi, X.-Y., Zhang, C.-S., Wang, X.-L., 2014. Increased nutrient loads from the Changjiang (Yangtze) River have led to increased Harmful Algal Blooms. Harmful Algae 39, 92–101. https://doi.org/10.1016/j.hal.2014.07.002.

Liu, K.-K., Yan, W., Lee, H.-J., Chao, S.-Y., Gong, G.-C., Yeh, T.-Y., 2015. Impacts of increasing dissolved inorganic nitrogen discharged from Changjiang on primary production and seafloor oxygen demand in the East China Sea from 1970 to 2002. J. Mar. Syst. 141, 200–217. https://doi.org/10.1016/j.jmarsys.2014.07.022.

Liu, Z., Gan, J., Wu, H., Hu, J., Cai, Z., Deng, Y., 2021. Advances on coastal and estuarine circulations around the Changjiang estuary in the recent decades (2000−2020). Front. Mar. Sci. 8, 615929 https://doi.org/10.3389/fmars.2021.615929.

Millero, F.J., Graham, T.B., Huang, F., Bustos-Serrano, H., Pierrot, D., 2006. Dissociation constants of carbonic acid in seawater as a function of salinity and temperature. Mar. Chem. 100 (1–2), 80–94. https://doi.org/10.1016/j.marchem.2005.12.001.

Ni, X., Huang, D., Zeng, D., Zhang, T., Li, H., Chen, J., 2016. The impact of wind mixing on the variation of bottom dissolved oxygen off the Changjiang Estuary during summer. J. Mar. Syst. 154, 122–130. https://doi.org/10.1016/j.jmarsys.2014.11.010.

Pierrot, D., Lewis, E., Wallace, W.R., 2006. MS Excel Program Developed for $CO_2$ System Calculations, ORNL/CDIAC-105a. Carbon Dioxide Information Analysis Center, Oak Ridge National Laboratory, U.S. Department of Energy, Oak Ridge, Tennessee.

Rabalais, N.N., Turner, R.E., Wiseman, W.J., 2002. Gulf of Mexico hypoxia, aka "The dead zone". Annu. Rev. Ecol. Evol. Syst. 33, 235–263. https://doi.org/10.1146/annurev.ecolsys.33.010802.150513.

Rabalais, N.N., Diaz, R.J., Levin, L.A., Turner, R.E., Gilbert, D., Zhang, J., 2010. Dynamics and distribution of natural and human-caused hypoxia. Biogeosciences 7 (2), 585–619. https://doi.org/10.5194/bg-7-585-2010.

Redfield, A.C., Ketchum, B.H., Richards, B.H., 1963. In: Hill, M.N. (Ed.), The Influence of Organisms on the Composition of Seawater in the Sea, vol. 2. Interscience Publisher, New York, pp. 26–77.

Tseng, C.M., Shen, P.-Y., Liu, K.-K., 2014. Synthesis of observed air-sea $CO_2$ exchange fluxes in the river-dominated East China Sea and improved estimates of annual and seasonal net mean fluxes. Biogeosciences 11, 3855–3870. https://doi.org/10.5194/bg-11-3855-2014.

Waldbusser, G.G., Hales, B., Langdon, C.J., Haley, B.A., Schrader, P., Brunner, E.L., Gray, M.W., Miller, C.A., Gimenez, I., 2015. Saturation-state sensitivity of marine bivalve larvae to ocean acidification. Nat. Clim. Change 5 (3), 273–280. https://doi.org/10.1038/nclimate2479.

Wang, S.L., Chen, C.T.A., Hong, G.H., Chung, C.S., 2000. Carbon dioxide and related parameters in the East China Sea. Cont. Shelf Res. 20 (4–5), 525–544.

Wang, B., Wei, Q., Chen, J., Xie, L., 2012. Annual cycle of hypoxia off the Changjiang (Yangtze River) Estuary. Mar. Environ. Res. 77, 1–5. https://doi.org/10.1016/j.marenvres.2011.12.007.

Wang, H., Dai, M., Liu, J., Kao, S.-J., Zhang, C., Cai, W.-J., Wang, G., Qian, W., Zhao, M., Sun, Z., 2016. Eutrophication-driven hypoxia in the East China Sea off the Changjiang estuary. Environ. Sci. Technol. 50 (5), 2255–2263. https://doi.org/10.1021/acs.est.5b06211.

Wang, B., Chen, J., Jin, H., Li, H., Huang, D., Cai, W.-J., 2017. Diatom bloom-derived bottom water hypoxia off the Changjiang estuary, with and without typhoon influence. Limnol. Oceanogr. 62 (4), 1552–1569. https://doi.org/10.1002/lno.10517.

Wang, B., Xin, M., Wei, Q., Xie, L., 2018. A historical overview of coastal eutrophication in the China Seas. Mar. Pollut. Bull. 136, 394–400. https://doi.org/10.1016/j.marpolbul.2018.09.044.

Wang, H., Yan, H., Zhou, F., Li, B., Zhuang, W., Yang, Y., 2019. Dynamics of nutrient export from the Yangtze River to the East China Sea. Estuar. Coast. Shelf Sci. 229 https://doi.org/10.1016/j.ecss.2019.106415.

Wang, H., Yan, H., Zhou, F., Li, B., Zhuang, W., Shen, Y., 2020. Changes in nutrient transport from the Yangtze River to the East China Sea linked to the Three-Gorges Dam and water transfer project. Environ. Pollut. 256 https://doi.org/10.1016/j.envpol.2019.113376.

Wang, K., Cai, W.-J., Chen, J., Kirchman, D., Wang, B., Fan, W., Huang, D., 2021. Climate and human-driven variability of summer hypoxia on a large river-dominated shelf as revealed by a hypoxia index. Front. Mar. Sci. 8 https://doi.org/10.3389/fmars.2021.634184.

Wei, H., He, Y., Li, Q., Liu, Z., Wang, H., 2007. Summer hypoxia adjacent to the Changjiang Estuary. J. Mar. Syst. 67 (3–4), 292–303. https://doi.org/10.1016/j.jmarsys.2006.04.014.

Weiss, R.F., 1974. Carbon dioxide in water and seawater: the solubility of a non-ideal gas. Mar. Chem. 2, 203–215. https://doi.org/10.1016/0304-4203(74)90015-2.

Xiong, T.-Q., Wei, Q.-S., Zhai, W.-D., Li, C.-L., Wang, S.-Y., Zhang, Y.-X., Liu, S.-J., Yu, S.-Q., 2020. Comparing subsurface seasonal deoxygenation and acidification in the Yellow Sea and northern East China Sea along the north-to-south latitude gradient. Front. Mar. Sci. 7 https://doi.org/10.3389/fmars.2020.00686.

Xu, Y.-Y., Pierrot, D., Cai, W.-J., 2017. Ocean carbonate system computation for anoxic waters using an updated CO2SYS program. Mar. Chem. 195, 90–93. https://doi.org/10.1016/j.marchem.2017.07.002.

Xu, L., Yang, D., Greenwood, J., Feng, X., Gao, G., Qi, J., Cui, X., Yin, B., 2020a. Riverine and oceanic nutrients govern different algal bloom domain near the Changjiang estuary in summer. J. Geophys. Res.: Biogeosci. 125 (10), e2020JG005727 https://doi.org/10.1029/2020jg005727.

Xu, T., Shi, X., Wang, G., Liu, Y., Liu, S., Qiao, S., Yao, Z., Wang, X., Fang, X., Li, X., Cao, P., Liu, J., 2020b. Holocene sedimentary evolution and hypoxia development in the subaqueous Yangtze (Changjiang) Delta, China. Mar. Geol. 430 https://doi.org/10.1016/j.margeo.2020.106359.

Yang, D., Yin, B., Liu, Z., Feng, X., 2011. Numerical study of the ocean circulation on the East China Sea shelf and a Kuroshio bottom branch northeast of Taiwan in summer. J. Geophys. Res. 116 (C05), C05015 doi:05010.01029/02010JC006777.

Yao, Z., 2019. Dynamics of Carbon and Nutrients and Impact on Ocean Acidification in the Changjiang Estuary and the Adjacent East China Sea Shelf, Master if Science Thesis, 74 (in Chinese with English Abstract). Xiamen University, Xiamen.

Yuan, D., Li, Y., Wang, B., He, L., Hirose, N., 2017. Coastal circulation in the southwestern Yellow Sea in the summers of 2008 and 2009. Cont. Shelf Res. 143, 101–117. https://doi.org/10.1016/j.csr.2017.01.022.

Zeebe, R.E., Wolf-Gladrow, D., 2003. $CO_2$ in Seawater: Equilibrium, Kinetics, Isotopes, 346 pp.. Elsevier.

Zhang, J., Liu, S.M., Ren, J.L., Wu, Y., Zhang, G.L., 2007. Nutrient gradients from the eutrophic Changjiang (Yangtze River) Estuary to the oligotrophic Kuroshio waters and re-evaluation of budgets for the East China Sea Shelf. Prog. Oceanogr. 74 (4), 449–478. https://doi.org/10.1016/j.pocean.2007.04.019.

Zhang, J., Gao, S., Liu, G., Wang, H., Zhu, X., 2016. Modeling the impact of river discharge and wind on the hypoxia off Yangtze estuary. Nat. Hazards Earth Syst. Sci. 16, 2559–2576. https://doi.org/10.5194/nhess-16-2559-2016.

Zhang, W., Wu, H., Zhu, Z., 2018. Transient hypoxia extent off Changjiang River estuary due to mobile Changjiang River plume. J. Geophys. Res. Oceans 123 (12), 9196–9211. https://doi.org/10.1029/2018jc014596.

Zhang, W., Wu, H., Hetland, R.D., Zhu, Z., 2019. On mechanisms controlling the seasonal hypoxia hot spots off the Changjiang River estuary. J. Geophys. Res. Oceans 124 (12), 8683–8700. https://doi.org/10.1029/2019jc015322.

Zhang, W., Zhou, F., Huang, D., Chen, J., Zhu, J., 2023. Mechanisms controlling interannual variability of seasonal hypoxia off the Changjiang River estuary. J. Geophys. Res. Oceans 128 (10), e2023JC019996. https://doi.org/10.1029/2023jc019996.

Zhao, Y., Liu, J., Uthaipan, K., Song, X., Xu, Y., He, B., Liu, H., Gan, J., Dai, M., 2020. Dynamics of inorganic carbon and pH in a large subtropical continental shelf system: interaction between eutrophication, hypoxia, and ocean acidification. Limnol. Oceanogr. 65 (6), 1359–1379. https://doi.org/10.1002/lno.11393.

Zheng, J., Gao, S., Liu, G., Wang, H., Zhu, X., 2016. Modeling the impact of river discharge and wind on the hypoxia off Yangtze Estuary. Nat. Hazards Earth Syst. Sci. 16 (12), 2559–2576. https://doi.org/10.5194/nhess-16-2559-2016.

Zhou, F., Chai, F., Huang, D., Xue, H., Chen, J., Xiu, P., Xuan, J., Li, J., Zeng, D., Ni, X., Wang, K., 2017. Investigation of hypoxia off the Changjiang Estuary using a coupled

model of ROMS-CoSiNE. Prog. Oceanogr. 159, 237–254. https://doi.org/10.1016/j.pocean.2017.10.008.

Zhu, Z.-Y., Wu, H., Liu, S.-M., Wu, Y., Huang, D.-J., Zhang, J., Zhang, G.-S., 2017. Hypoxia off the Changjiang (Yangtze River) estuary and in the adjacent East China Sea: quantitative approaches to estimating the tidal impact and nutrient regeneration. Mar. Pollut. Bull. 125 (1–2), 103–114. https://doi.org/10.1016/j.marpolbul.2017.07.029.

Zhu, T., Xu, B., Guo, X., Wei, Q., Lian, E., Liu, P., Burnett, W.C., Yao, Q., Yu, Z., 2023. Submarine groundwater discharge and seasonal hypoxia off the Changjiang River Estuary. Acta Oceanol. Sin. 42 (8), 125–133. https://doi.org/10.1007/s13131-023-2256-9.